Study of Entropy Noise through a 2D Stator using CAA

Ariane Emmanuelli, Maxime Huet, Thomas Le Garrec, Sébastien Ducruix

Study of Entropy Noise through a 2D Stator using CAA

Ariane Emmanuelli* and Maxime Huet† and Thomas Le Garrec‡
DAAA, ONERA, Université Paris Saclay,
F-92322 Châtilllon, France

Sebastien Ducruix§
Laboratoire EM2C, CNRS, CentraleSupélec, Université Paris-Saclay,
3, rue Joliot Curie, 91192 Gif-sur-Yvette cedex, France

Interest in entropy noise is growing because of its contribution to aero-engine noise, as well as its impact on combustion instabilities, which in turn affect NO_x emissions in particular. In this study, the entropy noise generated in a 2D stator cascade is investigated using Computational AeroAcoustic (CAA) simulations with a Euler mean flow field. Both the acceleration of an entropy wave through the stator row, producing entropy noise, and the scattering of upstream and downstream propagating acoustic waves by the blade are investigated. The resulting transfer functions are compared to a model for compact turbines developed by Cumpsty and Marble [Proc. of the Royal Soc. of London A, 357, 1977] and they show good agreement. The noise levels resulting from a model currently under development will be compared to the transfer functions presented in this paper in the future.

I. Introduction

The contribution of combustion noise to the overall noise generated by turbofan engines is becoming increasingly significant as fan and jet noise are reduced. In addition, combustion noise can impact thermo-acoustic instabilities in the combustion chamber. As well as being destructive, their understanding can help reduce NO_x emissions. Present in all gas turbines, combustion noise is comprised of two distinct contributions: direct and indirect noise. The former originates from the fluctuations in the heat released by the flame in the combustion chamber. The latter is generated by the acceleration of heterogeneities resulting from combustion through the rest of the engine, namely the turbine stages and the nozzle. These heterogeneities may be compositional, vortical or entropic, leading to entropy noise which is the subject of this paper.

The basis on the theory of indirect combustion noise was established in the seventies when Marble and Candel developed a model for compact nozzles [1]. It was followed by the work of Cumpsty and Marble which led to a model for compact turbine stages [2]. Interest in indirect combustion noise has renewed in the last couple of decades. Numerical [3] [4] [5] [6] and experimental [7] [8] [9] studies first focused on the simpler nozzle configuration, but numerical studies of a turbine stage [10] [11] also validated Cumpsty and Marble's compact model. They highlighted the presence of shear dispersion attenuation mechanisms in the turbine [11] and suggested entropy noise remains nonetheless significant [10]. This was confirmed by recent experimental results [12]. Another experimental study which focused on the effect of hot streak migration, confirmed the temperature attenuation across the blades and showed the effect of hot streak injection position as well as the impact on secondary flow [13]. Although advances are made numerically and experimentally, such studies remain complex and costly. Analytical investigations are a solution. Their low computational cost may also enable entropy noise to be taken into account in an industrial context. Modelling has mainly focused on the nozzle configuration. Marble and Candel's compact model gave way to many extensions in 1D, in particular to nozzles of arbitrary shapes and the non-linear regime [14] [15] [16] [17] [18]. The model CHEOPS-Nozzle was developed to take 2D radial variations into account [19] [20], and showed that 1D models are only valid at low frequency because entropy wave distortion greatly affects results in the rest of the frequency range [21].

The objective of this study is to build a reference case using Computational AeroAcoustics (CAA) to investigate the entropy noise generated in a 2D stator cascade. The resulting noise levels will be compared to those obtained with a

*PhD student, Department of Aerodynamics, Aeroelasticity and Acoustics, ONERA - the French Aerospace Lab, ariane.emmanuelli@onera.fr
†Research Scientist, Department of Aerodynamics, Aeroelasticity and Acoustics, ONERA - the French Aerospace Lab, maxime.huet@onera.fr
‡Research Scientist, Department of Aerodynamics, Aeroelasticity and Acoustics, ONERA - the French Aerospace Lab, thomas.le_garrec@onera.fr
§CNRS Senior Researcher, Laboratoire EM2C, CNRS and CentraleSupélec, Université Paris Saclay, sebastien.ducruix@centralesupelec.fr.

model which is currently under development, based on CHEOPS-Nozzle. After describing the chosen case, numerical and post-processing methods will be presented, and the entropy noise results will be discussed in a third section.

II. Case presentation

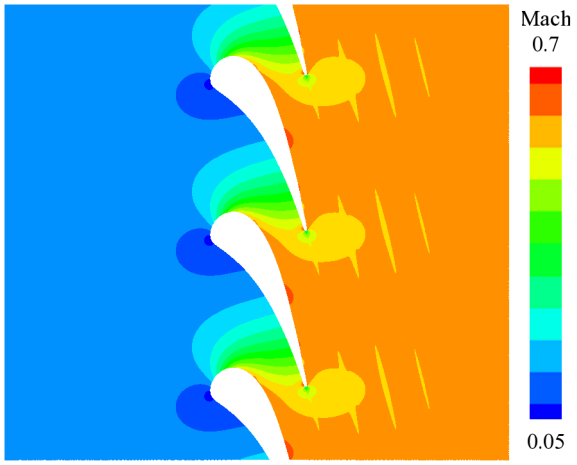

Fig. 1 Contour of the Mach number.

The geometry chosen for this application case is based on the stator used for the European-FP7 project RECORD [22] [23] [24], during which entropy noise was studied for the full turbine stage using the high-pressure turbine test-rig at Politecnico di Milano for both subsonic and supersonic operating points. The subsonic conditions are used in the present study, and the domain consists of a 2D profile extracted at 50% of the blade height, with lateral periodic boundaries and regions of length of about 20 axial-chords upstream and downstream for post-processing reasons. The mean flow field is simulated using the ONERA software Cedre [25], developed for energetics and propulsion applications. The fluid is considered inviscid and calorically perfect (constant heat capacity c_p). The Euler equations are solved on an unstructured mesh and simulations are run for air with a heat capacity ratio $\gamma = 1.4$. Spatial discretisation is of second order, and a pseudo-transient first order implicit scheme is used in time. The inlet temperature is set to 322 K, the inlet velocity to 42 m/s in the axial direction and the outlet pressure is 109216 Pa in accordance with the subsonic operating point of Politecnico di Milano's experimental study. The Mach number reaches 0.66 at the throat and its evolution is shown in Fig. 1. Note that this geometry generates strong acceleration and turning of the flow.

The objective is to investigate the entropy noise generated by the acceleration of a normalised plane entropy wave

$$\sigma = s'/c_p \tag{1}$$

though this mean flow field. Figure 2 shows the different waves involved. The axial direction is noted x and the azimuthal direction y. Indices 1 and 2 describe the inlet and outlet positions, while exponents $-$ and $+$ relate to acoustic waves travelling in the upstream and downstream directions respectively. The stator is forced with an incoming entropy wave σ_1, which generates the normalised transmitted and reflected acoustic waves ${P_2}^+$ and ${P_1}^-$. In the case where the pressure and velocity fluctuations p' and u' are purely acoustic, they may be expressed with the Riemann invariants:

$$P^+ = \frac{p^+}{\gamma p_0} = \frac{1}{2}\left(\frac{p'}{\gamma p_0} + \frac{u'}{c_0}\right) \tag{2}$$

$$P^- = \frac{p^-}{\gamma p_0} = \frac{1}{2}\left(\frac{p'}{\gamma p_0} - \frac{u'}{c_0}\right) \tag{3}$$

In addition, ${P_1}^+$ and ${P_2}^-$ are waves potentially originating from the reflection of ${P_1}^-$ and ${P_2}^+$ on the inlet and outlet boundaries of the domain respectively. The noise generated by the acceleration of the entropy wave σ_1 is studied using the thermo-acoustic transfer functions (TATF) $[{P_1}^-/\sigma_1]$ and $[{P_2}^+/\sigma_1]$, which caracterise the downstream and upstream

propagating waves, respectively. The scattering of acoustic waves by the stator is also investigated. To do so, acoustic waves are injected through the domain boundaries in additional simulations. Two cases are of interest: acoustic forcing from upstream with a wave P_1^+, and downstream forcing for which the wave P_2^- is injected. In the same way as for the TATF, the results can be analysed using the transfer functions $[P_1{}^-/P_1{}^+]$, $[P_2{}^+/P_1{}^+]$, $[P_2{}^+/P_2{}^-]$ and $[P_2{}^+/P_2{}^-]$. All six of these transfer functions will be discussed in section IV.

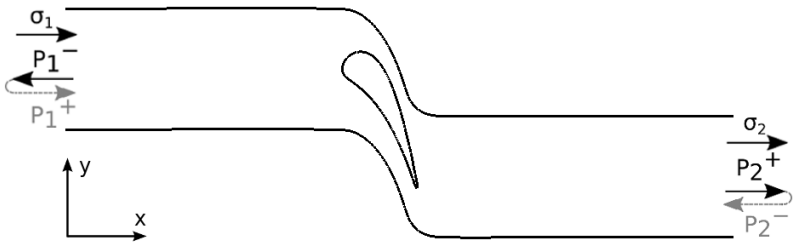

Fig. 2 Diagram of the waves propagating in the stator.

III. Numerical methods

A. CAA

The ONERA Computational AeroAcoustics (CAA) code *sAbrinA_v*0 [26] [27] is used for entropy wave convection and acoustic generation and propagation. The linearised Euler equations are solved in the time domain with a perturbation form of the conservative variables built using the mean flow and a disturbance field. A sixth order finite difference scheme is used combined with tenth order explicit filtering in space to avoid numerical dispersion and dissipation effects, and a third order explicit compact Runge-Kutta scheme is applied in time. The mesh is 2D structured, made of eight domains and 260000 points. The mean flow field described in section II is interpolated onto it. The mesh is dimensioned to have at least 20 points per acoustic or entropic wavelength, which is sufficient to propagate waves without significant numerical error in amplitude or in phase. A time step of 1.67×10^{-7} second is chosen so that the CFL reaches a maximum at 0.78.

The boundary conditions derived by Tam et al. [28] [29] from the asymptotic solutions of the linearised Euler equations are used both to ensure the almost perfectly non-reflective behaviour of the boundaries and to inject plane waves into the domain. As the linearised equations are solved, the computation of the noise levels at all frequencies considered is achieved with limited numerical cost by running a single simulation for each type of injected wave with multi-harmonic forcing varying from 100 Hz to 1000 Hz with a step of 100 Hz. Two harmonic simulations with entropy forcing at 100 Hz and 1000 Hz are also run to validate the numerical methodology. The resulting harmonic and multi-harmonic TATF are in good accordance as shown in Fig. 3.

B. Post-processing

Wave separation. The time signals obtained with *sAbrinA_v*0 must be post-processed to construct the acoustic waves. The Riemann invariants can give these directly under the condition pressure and velocity fluctuations are of acoustic origin only. However, in this particular case velocity fluctuations u' are not purely acoustic but also include a contribution from vorticity perturbations [30]. This is visible in Fig. 5 which also shows pressure fluctuations p' remain one-dimensional and purely acoustic. A direct mode matching wave separation method based solely on the pressure fluctuations can therefore be used [31]. In the harmonic regime, it writes:

$$p' = p'^{+} + p'^{-} \tag{4}$$

$$\frac{\partial p'}{\partial x} = -ik_x^+ p'^{+} - ik_x^- p'^{-} \tag{5}$$

where p'^- and p'^+ are the pressure fluctuations associated with the upstream and downstream propagating acoustic waves respectively, and the wavenumbers are expressed as:

$$k_x^+ = \frac{\omega}{u_0 + c_0} \tag{6}$$

$$k_x^- = \frac{\omega}{u_0 - c_0} \tag{7}$$

where ω is the angular frequency, u_0 the mean axial velocity and c_0 is the velocity of sound. The derivatives are evaluated using a finite difference scheme. Eqs. (4) and (5) form a linear system that can easily be solved to provide p'^+ and p'^-. To reduce numerical errors, the wave separation process is achieved for several planes in the upstream and downstream regions. The waves are then phase-shifted to a reference plane in each zone (the domain inlet for waves noted 1, and the outlet for position 2) before averaging and construction of the TATF.

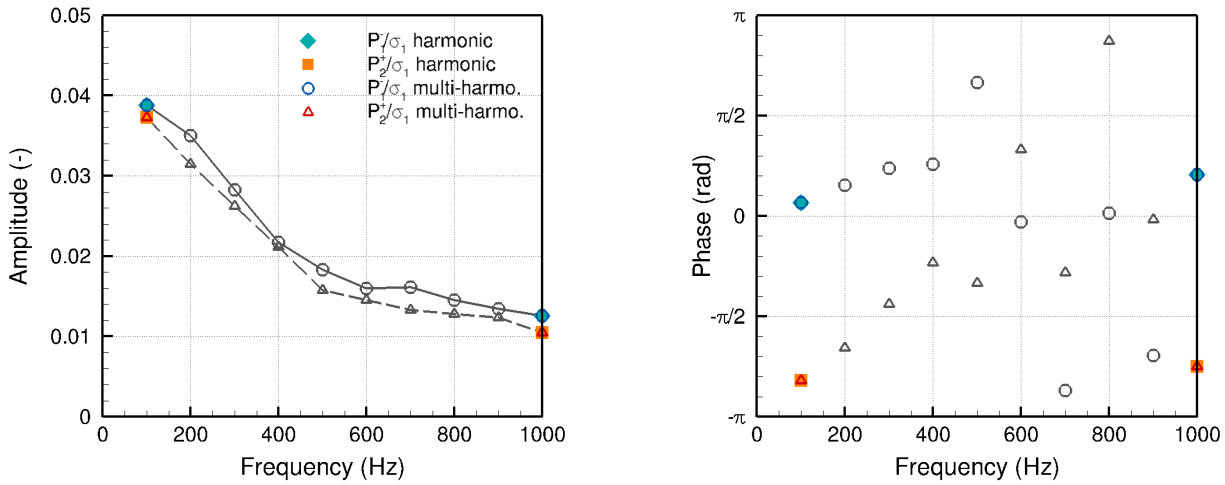

Fig. 3 Amplitude (left) and phase (right) of upstream (blue) and downstream (red) TATF obtained using harmonic and multi-harmonic simulations (data at frequencies not simulated with harmonic forcing is shown in grey).

Non-reflective post-processing. As the boundary conditions used may not be perfectly non-reflective, the post-processing described in this paragraph is used to cancel out any wave reflection arising from numerical errors. This is achieved by using results given by entropic forcing, upstream acoustic forcing and downstream acoustic forcing simulations, and by considering the acoustic transfer functions $[P_1{}^-/P_1{}^+]$, $[P_2{}^+/P_1{}^+]$, $[P_2{}^+/P_2{}^-]$ and $[P_2{}^+/P_2{}^-]$ as well as the TATF $[P_1{}^-/\sigma_1]$ and $[P_2{}^+/\sigma_1]$. The following system of six equations and six unknowns may be solved to obtain the non-reflective transfer functions:

$$P_1{}^-(\sigma_1) = \left[\frac{P_1{}^-}{\sigma_1}\right]_{nr} \sigma_1(\sigma_1) + \left[\frac{P_1{}^-}{P_1{}^+}\right]_{nr} P_1{}^+(\sigma_1) + \left[\frac{P_1{}^-}{P_2{}^-}\right]_{nr} P_2{}^-(\sigma_1) \tag{8}$$

$$P_2{}^+(\sigma_1) = \left[\frac{P_2{}^+}{\sigma_1}\right]_{nr} \sigma_1(\sigma_1) + \left[\frac{P_2{}^+}{P_1{}^+}\right]_{nr} P_1{}^+(\sigma_1) + \left[\frac{P_2{}^+}{P_2{}^-}\right]_{nr} P_2{}^-(\sigma_1) \tag{9}$$

$$P_1{}^-(P_1{}^+) = \left[\frac{P_1{}^-}{\sigma_1}\right]_{nr} \sigma_1(P_1{}^+) + \left[\frac{P_1{}^-}{P_1{}^+}\right]_{nr} P_1{}^+(P_1{}^+) + \left[\frac{P_1{}^-}{P_2{}^-}\right]_{nr} P_2{}^-(P_1{}^+) \tag{10}$$

$$P_2^+(P_1^+) = \left[\frac{P_2^+}{\sigma_1}\right]_{nr} \sigma_1(P_1^+) + \left[\frac{P_2^+}{P_1^+}\right]_{nr} P_1^+(P_1^+) + \left[\frac{P_2^+}{P_2^-}\right]_{nr} P_2^-(P_1^+) \quad (11)$$

$$P_1^-(P_2^-) = \left[\frac{P_1^-}{\sigma_1}\right]_{nr} \sigma_1(P_2^-) + \left[\frac{P_1^-}{P_1^+}\right]_{nr} P_1^+(P_2^-) + \left[\frac{P_1^-}{P_2^-}\right]_{nr} P_2^-(P_2^-) \quad (12)$$

$$P_2^+(P_2^-) = \left[\frac{P_2^+}{\sigma_1}\right]_{nr} \sigma_1(P_2^-) + \left[\frac{P_2^+}{P_1^+}\right]_{nr} P_1^+(P_2^-) + \left[\frac{P_2^+}{P_2^-}\right]_{nr} P_2^-(P_2^-) \quad (13)$$

The different quantities result from the forcing given in parenthesis, and the subscript *nr* indicates that the transfer functions are non-reflective.

IV. Results

The noise levels computed using the CAA approach described above are presented in this section. As the plane entropic wave injected into the domain is accelerated through the stator (recall the mean flow Fig 1) it is heavily deformed as illustrated in Fig 4. It is both chopped by the blade row and turned with the flow. The acceleration and deformation of this wave is responsible for the generated entropy noise in the form of the pressure and velocity fluctuations presented in Fig 5. As noted in section IIIB, the pressure fluctuations are one-dimensional throughout the domain, but the velocity fluctuations are not downstream of the blade because of a coupling with the vortical mode as the entropy wave is accelerated [30]. One may also note the colour contour is saturated in this region where the velocity fluctuations are larger than acoustic amplitudes.

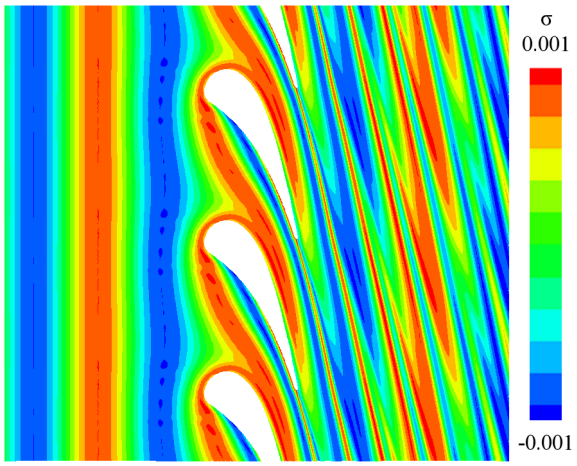

Fig. 4 Contour of normalised entropy fluctuations σ for harmonic forcing at 1000 Hz computed using CAA.

The resulting TATF $[P_1^-/\sigma_1]_{nr}$ and $[P_2^+/\sigma_1]_{nr}$ are presented in Fig. 6. The amplitude decreases sharply with frequency and there is a break in the curves around 500Hz after which the amplitude decreases very slowly. This evolution deserves further investigation. It is also worth noting the results for the upstream and downstream TATF are very close. The phase is presented in the range $[-\pi;\pi]$ as it is too poorly discretised to be unwrapped. This will however be possible in the prospect of comparison with analytical results, as their low computational cost allows greater sampling. The upstream acoustic transfer functions $[P_1^-/P_1^+]_{nr}$ and $[P_2^+/P_1^+]_{nr}$, and $[P_2^+/P_2^-]_{nr}$ and $[P_2^+/P_2^-]_{nr}$ resulting from downstream forcing are presented in Fig. 7 and Fig. 8 respectively. In addition, the compact solution, for which the dimension of the geometry is negligeable compared to the wavelength, is plotted for all three forcing cases. It was computed using the model developed by Cumpsty and Marble[2][11]. Although the CAA results could not be computed up to zero Hertz, they are in good accordance with the transfer functions resulting from the compact model for entropic forcing and both cases of acoustic forcing. Contrary to the entropic case, the amplitude of the acoustic transfer functions remains of the same order of magnitude as the compact solution over the range of frequencies considered, which can be explained by looking at the wavelengths involved. The smallest wavelengths (at 1000 Hz) upstream of the

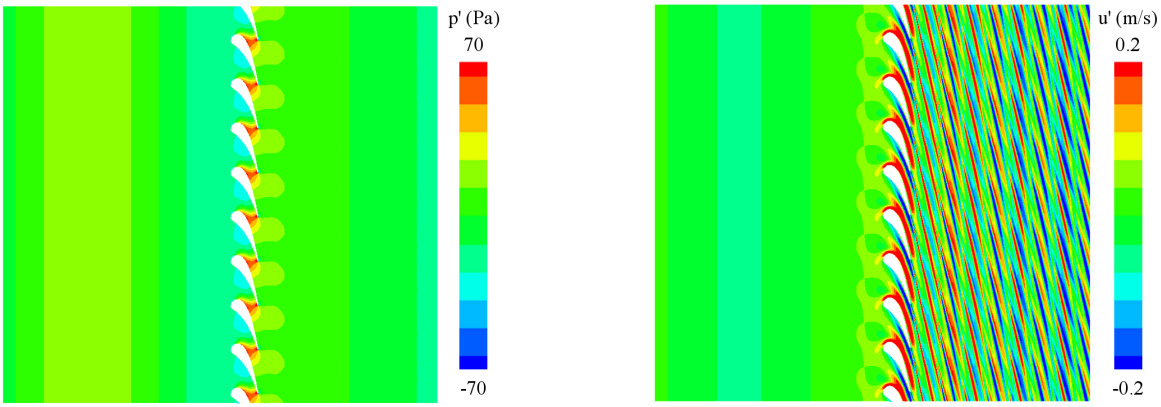

Fig. 5 Contour of pressure fluctuations p' (left) and axial velocity fluctuations u' (right) for harmonic forcing at 1000 Hz computed using CAA.

blade are between 0.3 and 0.4 m for the acoustic waves, whereas it is of only 0.04 m in the entropic case and the axial chord is 0.0306 m. The stator is therefore compact for both cases of acoustic forcing, whereas non-compactness affects the amplitude of the transfer functions significantly from about 200Hz.

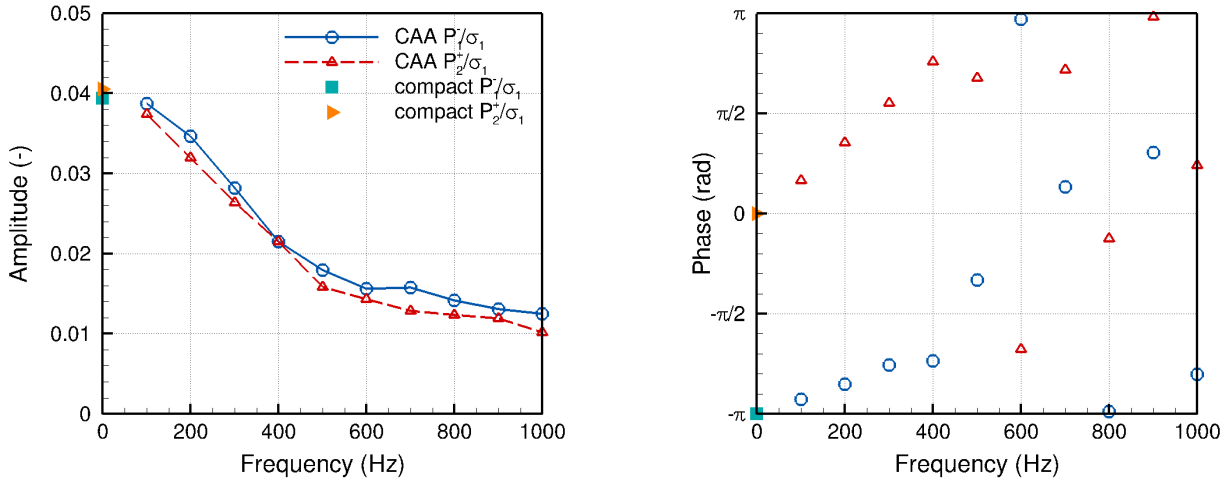

Fig. 6 Amplitude (left) and phase (right) of upstream and downstream non-reflective TATF computed using CAA and in the compact case[2].

V. Conclusions and prospects

A CAA reference case has been set up for the study of entropy noise in a 2D stator cascade. Noise levels were investigated for three forcing types: entropic, upstream acoustic and downstream acoustic. The resulting non-reflective transfer functions compare well with the compact solution[2]. The noise levels computed using a semi-analytical model currently under development will be compared with those presented in this paper. It follows the same main hypothesis as the model CHEOPS-Nozzle, in particular the assumption acoustic waves are one-dimensional, which has been verified

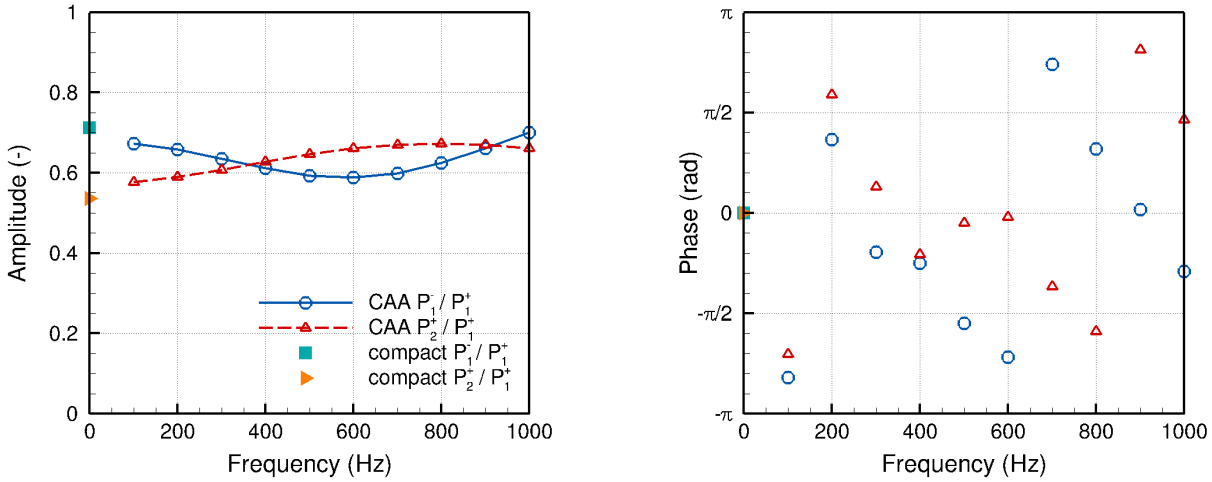

Fig. 7 Amplitude (left) and phase (right) of upstream and downstream non-reflective transfer functions resulting from the injection of a planar acoustic wave P_1^+ upstream using CAA, and in the compact case[2].

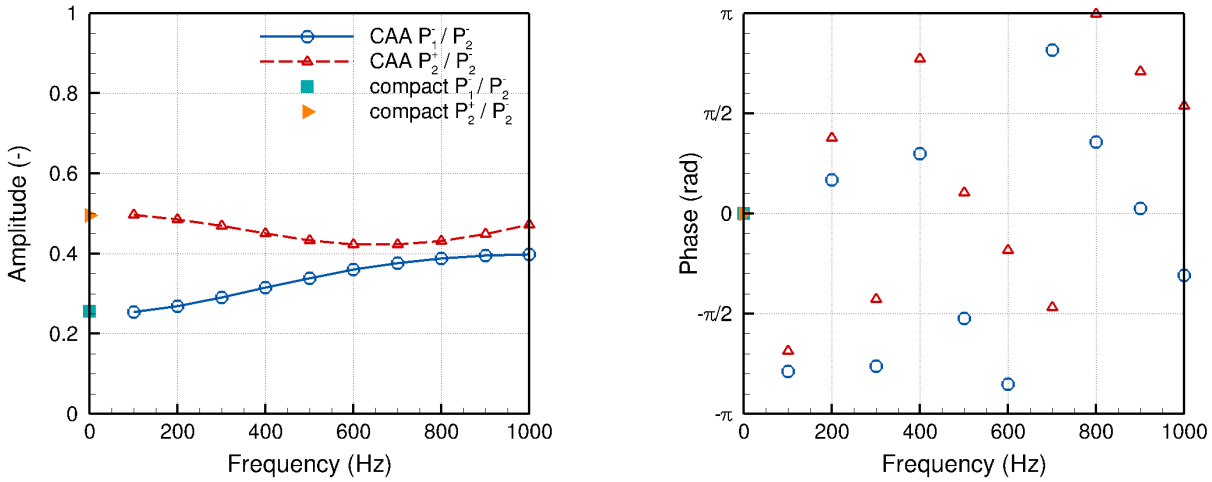

Fig. 8 Amplitude (left) and phase (right) of upstream and downstream non-reflective transfer functions resulting from the injection of a planar acoustic wave P_2^- downstream using CAA, and in the compact case[2].

in this paper. It is also based on the Euler equations, making a comparison with the present reference case all the more relevant. The 2D stator is studied in the context of a project aiming at developing a model for entropy noise through the turbine stages. In future studies, the model will be extended to the 3D stator and to the rotor. This will finally lead to a model for a full turbine stage, whose results could be compared to existing experimental data.

References

[1] Marble, F. E., and Candel, S. M., "Acoustic Disturbance from Gas Non-uniformities Convected Through a Nozzle," *Journal of Sound and Vibration*, Vol. 55, No. 2, 1977, pp. 225–243.

[2] Cumpsty, N. A., and Marble, F. E., "The Interaction of Entropy Fluctuations with Turbine Blade Rows; A Mechanism of Turbojet Engine Noise," *Proceedings of the Royal Society of London A*, Vol. 357, 1977, pp. 323–344.

[3] Richter, C., Panek, L., and Thiele, F., "On the Application of CAA - Methods for the Simulation of Indirect Combustion Noise," *11th AIAA/CEAS Aeroacoustics Conference, Aeroacoustics Conferences* , AIAA 2005–2919, 2005.

[4] Mühlbauer, B., Wiedenhorn, A., Liu, M., Noll, B., and Aigner, M., "Numerical Investigation of the Fundamental Mechanism of Entropy Noise Generation in Aero-engines," *Acta Acustica united with Acustica*, Vol. 95, No. 3, 2009, pp. 470–478.

[5] Leyko, M., Moreau, S., Nicoud, F., and Poinsot, T., "Numerical and Analitycal Modelling of Entropy Noise in a Supersonic Nozzle with a Shock," *Journal of Sound and Vibration*, Vol. 330, No. 16, 2011, pp. 3944–3958.

[6] Becerril, C., Moreau, S., Bauerheim, M., Gicquel, L., and Poinsot, T., "Numerical Investigation of Combustion Noise: The Entropy Wave Generator," *22nd AIAA/CEAS Aeroacoustics Conference, Aeroacoustics Conferences* , AIAA 2016–2830, 2016.

[7] Bake, F., Richter, C., Mühlbauer, B., Kings, N., Röhle, I., Thiele, F., and Noll, B., "The Entropy Wave Generator (EWG): a Reference Case on Entropy Noise," *Journal of Sound and Vibration*, Vol. 326, No. 3–5, 2009, pp. 574–598.

[8] Knobloch, K., Werner, T., and Bake, F., "Entropy Noise Generation and Reduction in a Heated Nozzle Flow," *21st AIAA/CEAS Aeroacoustics Conference, AIAA AVIATION Forum*, AIAA 2015–2818, 2015.

[9] Kings, N., Tao, W., Scouflaire, P., Richecoeur, F., and Ducruix, S., "Experimental and Numerical Investigation of Direct and Indirect Combustion Noise in a Lean Premixed Laboratory Swirled Combustor," *ASME Turbo Expo*, GT2016–57848, 2016.

[10] Duran, I., and Moreau, S., "Numerical simulation of acoustic and entropy waves propagating through turbine blades," *19th AIAA/CEAS Aeroacoustics Conference*, AIAA 2013-2102, 2013.

[11] Leyko, M., Moreau, S., Nicoud, F., and Poinsot, T., "Simulation and Modelling of the Waves Transmission and Generation in a Stator Blade Row in a Combustion-Noise Framework," *Journal of Sound and Vibration*, Vol. 333, No. 23, 2014, pp. 6090–6106.

[12] Knobloch, K., Neuhaus, L., Bake, F., Gaetani, P., and Persico, G., "Experimental Assessment of Noise Generation and Transmission in a High-Pressure Transonic Turbine Stage," *Journal of Turbomachinery*, Vol. 139, 2017.

[13] Gaetani, P., and Persico, G., "Hot Streak Evolution in an Axial HP Turbine Stage," *International Journal of Turbomachinery Propulsion and Power*, Vol. 2, 2017.

[14] Huet, M., and Giauque, A., "A Nonlinear Model for Indirect Combustion Noise Through a Compact Nozzle," *Journal of Fluid Mechanics*, Vol. 733, 2013, pp. 268–301.

[15] Huet, M., "Nonlinear Indirect Combustion Noise for Compact Supercritical Nozzle Flows," *Journal of Sound and Vibration*, Vol. 374, 2016, pp. 211–227.

[16] Moase, W., Brear, M. J., and Manzie, C., "The Forced Response of Chocked Nozzles and Supersonic Diffusers," *Journal of Fluid Mechanics*, Vol. 585, 2007, pp. 281–304.

[17] Giauque, A., Huet, M., and Cléro, F., "Analytical Analysis od Indirect Combustion Noise in Subcritical Nozzles," *Journal of Engineering for Gas Turbines and Power*, Vol. 134, No. 11 1102, 2012.

[18] Duran, I., and Moreau, S., "Solution of the Quasi-one-dimensional Linearized Euler Equations Using Flow Invariants and the Magnus Expansion," *Journal of Fluid Mechanics*, Vol. 723, 2013, pp. 190–231.

[19] Zheng, J., Huet, M., Giauque, A., Cléro, F., and Ducruix, S., "A 2D-axisymmetric Analytical Model for the Estimation of Indirect Combustion Noise in Nozzle Flows," *21st AIAA/CEAS Aeroacoustics Conference, AIAA AVIATION Forum* , AIAA 2015-2974, 2015.

[20] Zheng, J., "Analytical and Numerical Study of the Indirect Combustion Noise Generated by Entropy Disturbances in Nozzle Flows," PhD Thesis, Université Paris Saclay, 2016.

[21] Emmanuelli, A., Huet, M., Garrec, T. L., and Ducruix, S., "CAA Study of Entropy Noise in Nozzle Flow for the Validation of a 2D Semi-analytical Model," *ASME Turbo Expo*, GT2017-63640, 2017.

[22] Knobloch, K., Neuhaus, L., Bake, F., Gaetani, P., and Persico, G., "Experimental Essessment of Noise Generation and Transmission in a High-pressure Transonic Turbine Stage," *ASME Turbo Expo*, GT2016-57209, 2016.

[23] Knobloch, K., Holewa, A., Guérin, S., Mahmoudi, Y., Hynes, T., and Bake, F., "Noise Transmission Characteristics of a High Pressure Turbine Stage," *22nd AIAA/CEAS Aeroacoustics Conference, Aeroacoustics Conferences*, AIAA 2016-3001, 2016.

[24] Bake, F., Gaetani, P., Persico, G., Neuhaus, L., and Knobloch, K., "Indirect Noise Generation in a High Pressure Turbine Stage," *22nd AIAA/CEAS Aeroacoustics Conference, Aeroacoustics Conferences*, AIAA 2016-3001, 2016.

[25] Refloch, A., Courbet, B., Murrone, A., Villedieu, P., Laurent, C., Gilbank, P., Troyes, J., Tssé, L., Chaineray, G., Dargaud, J., Quémerais, E., and Vuillot, F., "CEDRE Software," *Aerospace Lab*, Vol. 2, 2011.

[26] Redonnet, S., Manoha, E., and Sagaut, P., "Numerical Simulations of Propagation of Small Perturbations Interacting with Flows and Solid Bodies," *7th AIAA/CEAS Aeroacoustics Conference, Aeroacoustics Conferences* , AIAA 2001-0222, 2001.

[27] Redonnet, S., "Numerical Study of Acoustic Installation Effects with a Computational Aeroacoustics Method," *AIAA Journal*, Vol. 48, No. 5, 2010, pp. 929–937.

[28] Tam, C., and Dong, Z., "Radiation and Outflow Boundary Conditions for Direct Computation of Acoustic and Flow Disturbances in a Nonuniform Mean Flow," *Journal of Computational Acoustics*, Vol. 4, No. 2, 1996, pp. 175–201.

[29] Tam, C., and Webb, J., "Dispersion-Relation-Preserving Finite Difference Schemes for Computational Acoustics," *Journal of Computational Physics*, Vol. 107, No. 2, 1993, pp. 262–281.

[30] Duran, I., and Morgans, A. S., "On the Reflection and Transmission of Circumferential Waves Through Nozzles," *Journal of Fluid Mechanics*, Vol. 773, 2015, pp. 137–153.

[31] Rienstra, S. W., and Hirschberg, A., *An Introduction to Acoustics*, Eindhoven University of Technology, 2011.